Journal of Power Sources 246 (2014) 167–177

Contents lists available at ScienceDirect

Journal of Power Sources

journal homepage: www.elsevier.com/locate/jpowsour

Review

Si/C hybrid nanostructures for Li-ion anodes: An overview

Maria Letizia Terranova [a], Silvia Orlanducci [a], Emanuela Tamburri [a], Valeria Guglielmotti [a], Marco Rossi [b,*]

[a] Dept. of Chemical Science and Technology – Minima Lab, University of Rome "Tor Vergata", Via della Ricerca Scientifica, Rome 00133, Italy
[b] Dept. of Basic and Applied Sciences for Engineering and Center for Nanotechnologies Applied to Engineering, Sapienza University of Rome, Via A. Scarpa 16, Rome 00161, Italy

HIGHLIGHTS

- The review regards an emerging and very hot area of research.
- Si/C nanomaterials have ideal properties for innovative and improved Li-ion battery anodes.
- The review present an overview of the methodologies proposed in the last decade for Si/C.
- The relationships between properties of Si/C at nanoscale and battery performance are discussed.
- Promising routes for the optimized fabrication of Si/C nanomaterials are reported.

ARTICLE INFO

Article history:
Received 7 April 2013
Received in revised form
1 July 2013
Accepted 15 July 2013
Available online

Keywords:
Si/C
Hybrid nanostructures
Li-ion batteries
Anodes
Green technologies

ABSTRACT

This review article summarizes recent and increasing efforts in the development of novel Li ion cell anode nanomaterials based on the coupling of C with Si. The rationale behind such efforts is based on the fact that the Si–C coupling realizes a favourable combination of the two materials properties, such as the high lithiation capacity of Si and the mechanical and conductive properties of C, making Si/C hybrid nanomaterials the ideal candidates for innovative and improved Li-ion anodes. Together with an overview of the methodologies proposed in the last decade for material preparation, a discussion on relationship between organization at the nanoscale of the hybrid Si/C systems and battery performances is given. An emerging indication is that the enhancement of the batteries efficiency in terms of mass capacity, energy density and cycling stability, resides in the ability to arrange Si/C bi-component nanostructures in pre-defined architectures. Starting from the results obtained so far, this paper aims to indicate some emerging directions and to inspire promising routes to optimize fabrication of Si/C nanomaterials and engineering of Li-ion anodes structures. The use of Si/C hybrid nanostructures could represents a viable and effective solution to the foreseen limits of present lithium ion technology.

1. Introduction

The Li-ion batteries, based on the intercalation concept proposed by M. Whittingham in the '70s, represent nowadays the highest performing secondary battery systems [1–3] and play an essential role in modern technologies, representing in particular the best battery technology now available for vehicles. They are commonly used in portable electronics and mobile communication devices and are now entering the markets of hybrid and electrical vehicles. Moreover, the ability to produce less expensive batteries with extremely reduced sizes and long cycle life will facilitate the adoption of many other "green" technologies, such as the solar cells. Expectations of convenience and long-living portable power urged to develop technological strategies that resulted in a net improvement of the batteries performances. These advances can be better appreciated if one considers that in the last decade the energy density has been improved 2 times. The energy density per unit area is a critical figure of merit for power modules, whereas for other applications, such as electrical vehicles, the density per unit weight is the key parameter. To reach high energy density the anode materials must combine high specific storage capacity and coulombic efficiency [4].

* Corresponding author.
E-mail addresses: marialetizia.terranova@roma2.infn.it (M.L. Terranova), silvia.orlanducci@uniroma2.it (S. Orlanducci), emanuela.tamburri@uniroma2.it (E. Tamburri), valeria.guglielmotti@uniroma2.it (V. Guglielmotti), marcorossi@uniroma1.it, marco.rossi@nanoshare.com (M. Rossi).

0378-7753/$ – see front matter © 2013 Published by Elsevier B.V.
http://dx.doi.org/10.1016/j.jpowsour.2013.07.065

For reversible intercalation of Li ions, commercial rechargeable batteries rely on anodes made by graphite, mainly in form of particles with sizes in the 15–20 micron range. Although the good performances of the graphite materials in terms of electronic conductivity, low electrochemical potential and coulombic efficiency (>95%), the low specific lithiation capacity (372 mAh g^{-1}) [5] limit the possibility to force up the efficiency and to meet the ever increasing requirements of our society. The current state-of-art technology based on the combination of a graphitic anode and of a Li-oxide or Li-phosphate cathode is approaching its limit both in mass capacity, usually expressed in Wh Kg^{-1}, and in energy density (Wh L^{-1}) [6,7]. In order to enhance the performances of such batteries, in the place of graphite several different anode materials with higher specific capacity of Li accommodation have been proposed. In re-envisioning materials for Li-ion intercalation good perspectives are offered by Al, Sn, Sb, Si. Without any doubt, the most promising element is Si, characterized by a high theoretical specific capacity (4008 mAh g^{-1}, corresponding to the formation of the $Li_{22}Si_5$ alloy) that is an order of magnitude beyond that offered by conventional graphite anodes [8–10].

However, the use of pure Si is hampered by the mechanical behaviour of the Si lattice that, under repeated expansion/contraction cycles – as the Li ions enter and leave the anode – undergoes up to 300% volume increase [11]. The stresses produced by the volume changes induce structural modifications of the Si phase and create damages in the solid-electrolyte interphase (SEI). The SEI is produced by the decomposition of the organic electrolytes on the electrode material. For a long cycle life the presence of an ionically conductive and electronically insulating stable SEI layer is critical. The Si shrinkage during the de-lithiation steps makes the SEI layer vulnerable to cracking and exfoliation, with breakage of electrical contact between active material and current collector and consequent rapid failing of the electrode [9,12].

Several strategies have been suggested in the last decade to reduce the limitations due to both the volume swelling under Li charging and the intrinsic low electrical conductivity of Si. It has been demonstrated that the use of three-dimensional nanoporous Si [13–15] could strongly enhance the cell capacity.

A much more pursued approach relies on the reduction of the dimensions of the Si phase and on the use of nanosized Si. Switching to nanomaterials, investigations have been focused on the use of Si in form of nanoparticles, nanowires, nanotubes and hollow particles [9]. All these Si nanostructures demonstrated improved kinetics of the Li ion transport and facilitated relaxation of the stress–strain associated to the insertion/extraction processes [16–24]. A nanocrystalline Si particle prepared by the methodology described in Ref. [22] is depicted in Fig. 1. Such preparation technique has proved to avoid particles aggregation and to preserve the size distribution of the as-produced Si entities. An interesting synthesis strategy is that one described by Yao et al. [25], namely the fabrication of interconnected Si hollow nanospheres. This architecture allowed to maintain high capacities over 700 cycles, the longer ever reported for a silicon anode.

The nanosized Si materials can give high capacities, but are not a concurrence to conventional graphite anodes, when cycle life and fading are considered. This fact can be rationalized considering that the large surface area of the nanostructured Si dramatically increases the occurrence of chemical reactions in the electrolytes. As an example, the widely used $LiPF_6$ electrolyte can be easily decomposed, with production of HF that in turn affects the surface chemistry of the electrodes and induces a severe etching of the Si phase [26].

To stabilize the SEI layers contacting the Si surface, many materials with intrinsic good conductivity have been tested [27–30]. Among the investigated coating materials, C demonstrated to be effective not only in stabilizing the SEI layers but also in enhancing the electronic conductivity of the Si-based anodes [31,32].

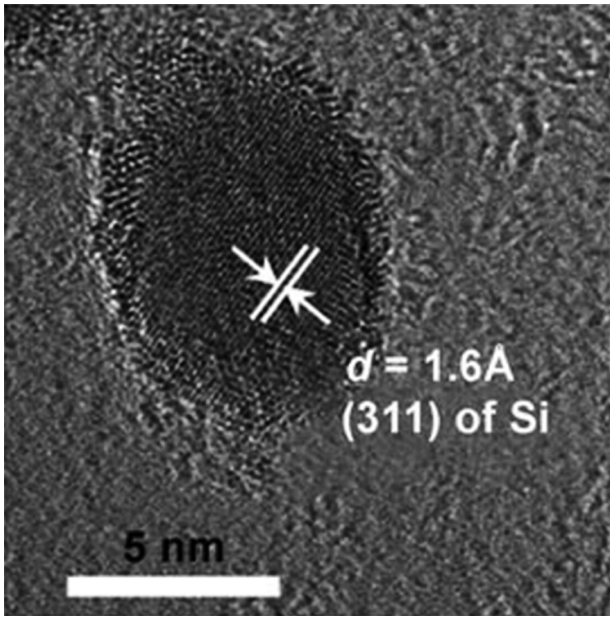

Fig. 1. TEM image of a nanocrystalline Si particle prepared using trimethyloctadecylammonium bromide surfactant (d = 5 nm). ©From Ref. [22].

However, if one considers individual materials, neither carbon nor the theoretically more efficient silicon is presently able to offer the reversible high-capacity and the long service life required to power modern multifunctional electronic devices.

Starting from about 1996, several studies addressed the shortcomings related to the use of micro- or nano-structured silicon coupled with carbon for battery anodes, thus realizing a favourable combination of the properties of the two materials [16,33–39]. The rationale of these researches is based on the fact that the mechanical properties of graphitic carbon, such as the elasticity, make it able to buffer the volume expansion of Si, whereas the high conductivity of C can efficiently complement the high lithiation capacity of Si [40].

The encouraging first results clearly showed that the coupling of C and Si in the anode materials would be a viable option for efficient charge and ion transport in rechargeable batteries. In this context it was observed that a key role in defining the anode performances is played by the structure and the mutual organization of the two components. As an example, an initial high capacity, but a lack of stability has been detected in the case of Si/C anodes prepared by decomposition of C and Si containing precursors or by mechanical mixing processes. The poor results have been imputed to the limited porosity available for accommodation of Si volume changes and to the lack of uniformity in the properties of the composites at the nanoscale. Much more promising results in terms of cycle stability were obtained using homogeneously distributed C and Si components and networks of interconnected pores [12,13,41,42].

In the search of new high-performance anode materials, a significant step is represented by the use of fabrication techniques at the nanoscale to produce designed Si/C nanocomposites addressing the limitations of all-C and all-Si battery anodes. Si/C heteronanomaterials, their nature, their use and almost spectacular envisaged capabilities, are a topic that is gaining a rather important place in the scientific literature. In the last few years there was an upsurge of papers mainly related to the technical developments that enable the production of various, sometimes unexpected, Si/C

hybrid nanostructures, with intriguing properties suitable for application in the battery technology. Researches of advanced materials for Li-ion battery anodes have to include a road map for materials preparation as well as structural/morphological/compositional and electrochemical investigations.

This review article surveys and discusses the methods proposed in the last decade for the production of hybrid Si/C systems suitable for the assembling of anodes in Li ion batteries. A short description of the main results obtained by using the various materials is also given.

For the sake of clarity, the paper is organized with the following sections: 1) Si/C mixing by milling; 2) porous Si/C systems; 3) Si coating of C nanostructures; 4) C coating of Si structures; 5) core–shell Si/C systems. The final section 6) reports *in situ* characterizations of Si/C hetero materials.

1.1. Si/C mixing by milling

High energy ball milling of mixtures of silicon and various carbon materials under noble gas atmosphere was one of the first proposed synthetic route, and is a methodology still widely employed to prepare C/Si composites and nanocomposites. The process is followed in general by a pyrolysis step [43–45].

A comparison between pyrolyzed blends of Si sub-micro particles with several organic precursors was performed in Ref. [45]. The comparison between the various Si-containing disordered carbon materials obtained using different precursors evidenced the superior behaviour of poly(vinylidene fluoride) (PVDF). The strong etching of Si induced by HF during the pyrolysis helps in producing a compact interface between Si and C, with suppression of the Si pulverization during the charge–discharge battery cycles. Fig. 2 reports a TEM image of the interface between Si and C in the pyrolyzed Si/PVDF composite. The presence of such a compact interface provides efficient electron paths. The material configuration allowed reaching a 75% of capacity retention after 50 cycles.

A study on the relationship between size of Si micro particles, chlorine content in the chlorinated polyethylene precursor, carbon content of the composites and electrochemical performances has been reported in Ref. [46]. In this case the chlorine content in the carbon precursor was found to have no influence on the cycling performances.

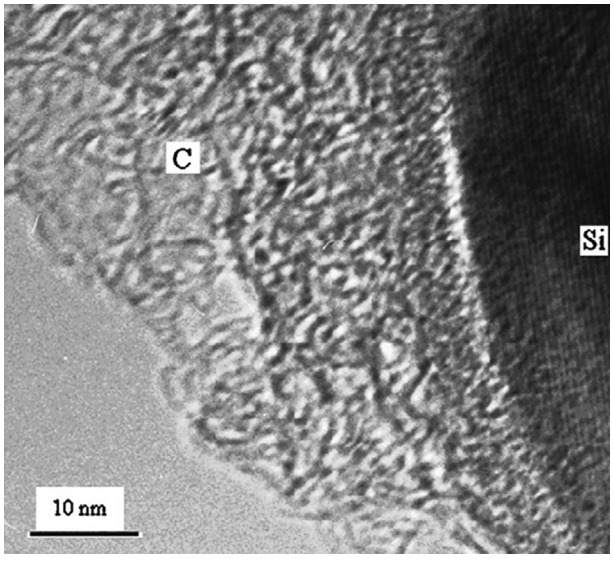

Fig. 2. TEM image showing the cross section of the Si/PVDF composite pyrolyzed at 900 °C. ©From Ref. [45].

Composites were also obtained by dispersing fine Si particles and carbonaceous mesophase spherules in pyrolyzed petroleum pitch [47]. The structural analysis demonstrated that pitch pyrolysis produces micropores in the composite and that the Si phase is converted from crystalline to amorphous after the first cycle. The investigation of Uono et al. [48] on Si/graphite/pitch cokes systems obtained by milling and heat treatments, demonstrated that appropriate sizes of Si and graphite particles are needed in order to keep low the irreversible capacity.

Si-graphite nanocomposites have been prepared by ball milling using natural graphite and silicon [49]. The final material consisted in Si particles intercalated between the lamellar structure of the graphite flakes. A limited improvement of the cyclability can be obtained thanks to the decrease of the volume changes for the occluded Si particles, even if the loose connections among the flaked graphite particles do not allow a complete control of the volume changes. Different types of composite electrodes were obtained mixing graphite and nanosilicon prepared by pyrolysis of SiH_4 [11]. The measured capacity of about 1000 mAh g^{-1} seems to indicate that the nanosilicon produced by such a methodology has reached the theoretically predicted intercalation capacity for Li ions. The cycling stability is likely related to the large amount of graphite mixed to the nanosilicon. The paper by Zuo et al. [50] reports a scheme of the structural and morphological evolution of Si/C/graphite materials before and after lithiation/delithiation cycling. Using Si/C/graphite hybrids prepared by dispersing Si and graphite particles into a pyrolyzed phenol–formaldeyde resin, a reversible capacity up to 700 mAh g^{-1} was measured. The authors suggest that the role played by the graphite matrix is that of controlling the expansion of the small-sized Si particles, therefore increasing the mechanical stability of the anode material.

A further development along the line of Si/graphite composites was the adding of carbon nanotubes (CNT) [51–54]. The CNT, characterized by high electrical conductivity and high degree of resiliency, can moreover behave as a ductile host matrix able to accommodate the volume changes. Marked differences have been found in the anode characteristics depending on the preparation methods of the CNT–Si systems. In Ref. [51] the rather high initial Li intercalation capacity of the Si component (1500 mAh g^{-1}) could be partially maintained for 10 cycles only in the case of Cr-doped Si. In these experiments, the Si doping by Cr, B, or P makes intrinsically difficult to disentangle the contribution of CNT from the effects induced by the dopants. Multicomponent systems based on silicon/graphite/CNT [53] and silicon/CNT/pyrolytic carbon [54] were also tested. Fig. 3 shows the HRTEM images of Si/CNT and Si/CNT/C deposits. In both the experiments an improvement of the cyclability was evidenced.

1.2. Porous Si/C systems

Micro- and nano-porous Si/C complex structures have been also produced by proper material engineering procedures. Si/C porous composites were initially prepared by pyrolyzing mixtures composed by Si powders (average sizes: 0.7, 4 and 10 μm) with PVC or CPE (chlorinated polyethylene) [46].

Feng et al. [55] recently reported about a mechanochemical reaction between $SiCl_4$ and $Li_{13}Si_4$ under ball milling. A series of different nanoporous Si/C composite anode materials with outstanding electrochemical properties were prepared and tested. The best Si/C nanocomposite was characterized by an initial capacity of 1413 mAh g^{-1} and a 91% capacity retention after 100 cycles, at a current density of 100 mA g^{-1}. The good electrochemical performances have been rationalized on the basis of the open nanoporous structure and of the electronic and ionic conductivity of the carbon layers [55].

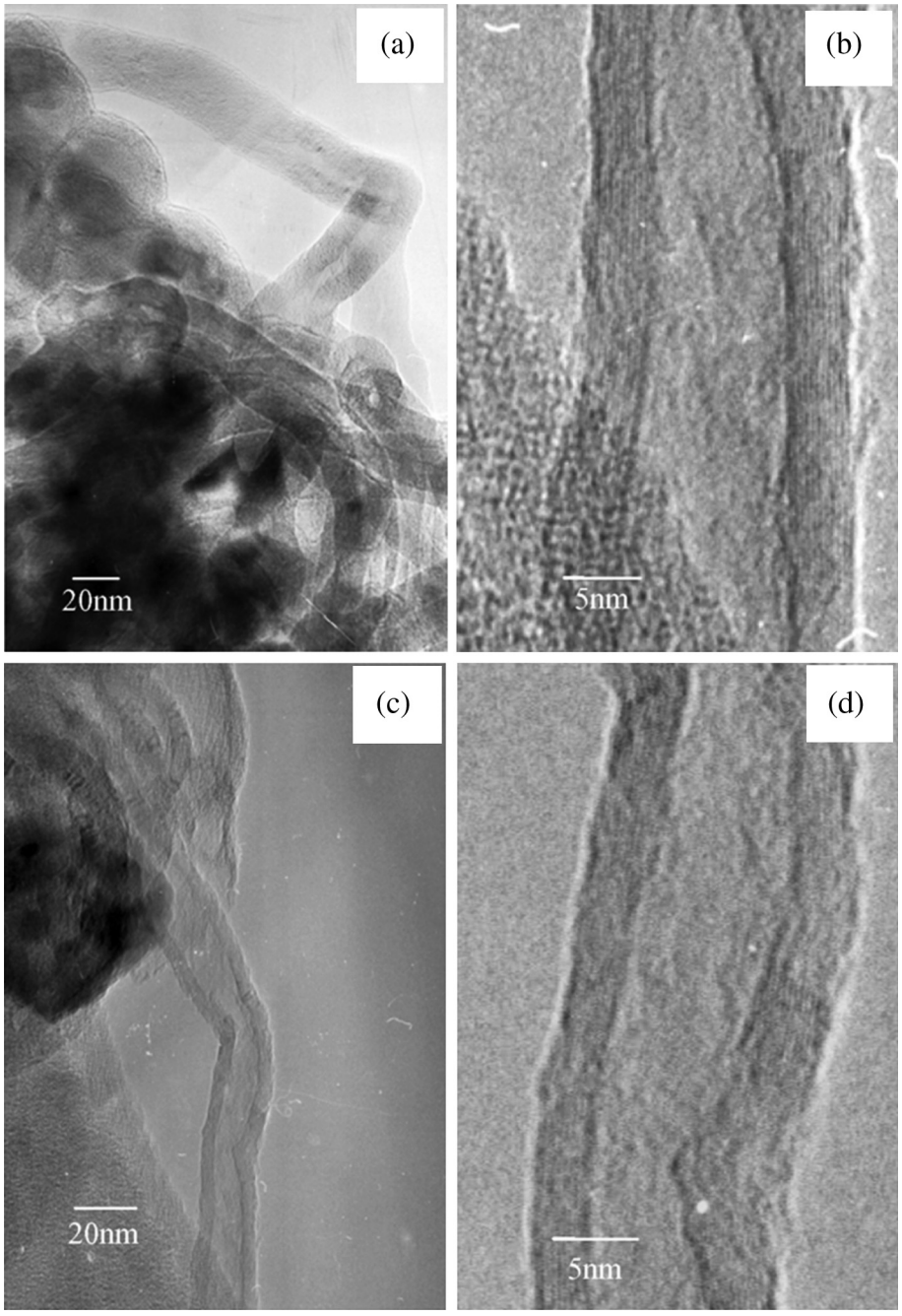

Fig. 3. HRTEM micrographs of (a–b) Si/CNT systems and (c–d) Si/CNT/C systems. ©From Ref. [54].

Another viable option to prepare Si/C anode materials is that of using porous carbon scaffold to support or incorporate Si nanostructures. Porous carbon scaffold Si anodes have been prepared by carbonization of Si–polyvinylidene fluoride directly deposited on the current collector using a slurry spray technique [56]. The carbon scaffold is characterized by a close-knit structure with a large number of nanosized pores distributed over the whole anode. The nanopores incorporate the Si particles, avoiding Si exfoliation in case of pulverization, and accommodating the strain/stress due the volume changes during lithiation. Using this anode material and different cycling rates good electrochemical performances were obtained, with a retained charge capacity of 60%–80% after 112–142 full cycles [56].

Nanoporous carbon matrices able to host silicon nanostructures were prepared by carbonization of viscous pitch using a silica nanoparticle template [57]. 1D Si nanostructures were selectively grown inside the empty channels of the carbon matrices by Au-catalyzed depositions based on a vapour-liquid-solid approach (Fig. 4). The interconnected porous network facilitated both the electron and ion transport. The performance test demonstrated a charge storage capacity of about 1600 mAh g^{-1} and good capacity retention.

Spheroidal carbon-coated Si nanocomposites with specific crystallographic features have been engineered by spray pyrolysis [58]. The starting material was a suspension of Si/citric acid/ethanol, the final material consisting in individual units with a crystalline Si core and an amorphous pyrolyzed carbon coating external layer.

Nanoporous Si/C micro/nanospheres have been recently taken into consideration as promising anode materials for Li-ion batteries.

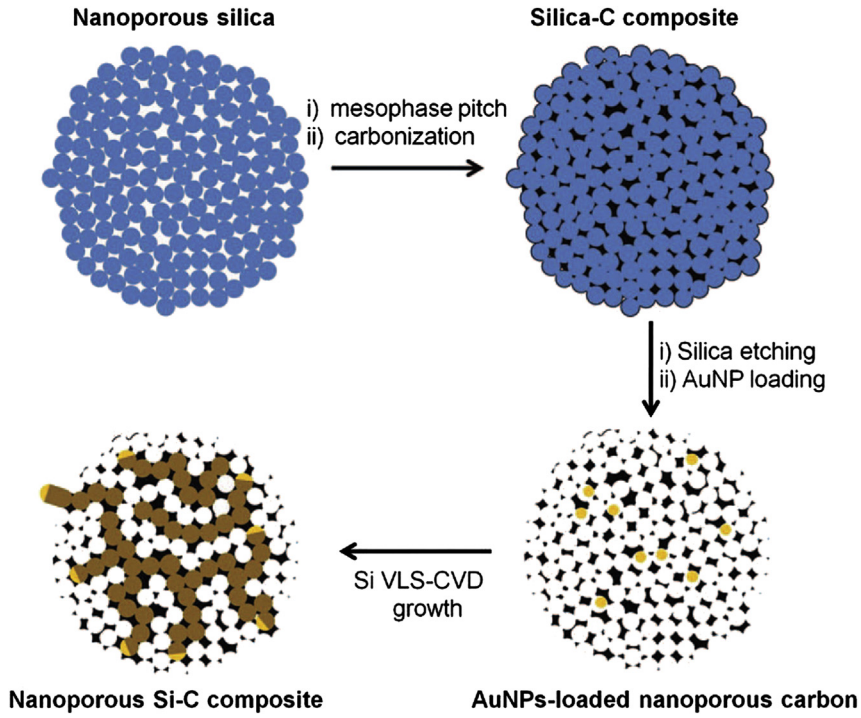

Fig. 4. Scheme of the fabrication of nanoporous Si/C composites. ©From Ref. [57].

The concept of micro-nanospheres can be realized following different synthetic routes. Yin et al. [59] designed and assembled Si/C nanoporous microspheres by a programmed procedure, starting from the electrospraying of aqueous solutions containing Si nanoparticles. The subsequent steps were calcinations, carbon coating by physical vapour deposition (PVD) and etching using hydrofluoric acid to enlarge the nanopores of the microspheres. The preparation methodology of Si/C nanoporous microspheres is given in Fig. 5. The stable structure of the microspheres provides an efficient accommodation of Si volume changes and stress release during cycles. The Si/C nanoporous microspheres exhibit remarkable enhancement of the cyclic and rate performances compared with Si nanoparticles.

Sponge-like Si–CNT structures with large areal mass loading (up to 8 mg cm^{-2}) have been prepared by incorporating Si into porous 3D CNT sponge-like structures [60]. The CNT sponges, prepared following the same procedure reported in Ref. [61], are used as highly conductive template for conformal deposition of Si by a chemical vapour deposition (CVD) process and formation of Si–CNT coaxial nanostructures. The amorphous Si shell (about 30 nm thickness) is the component that acts for Li storage. As illustrated in Fig. 6, each shell expands during lithiation in the radial direction through the Li-ion flow. During de-lithiation, however, if the sizes of the nanopores formed by tensile stresses exceed a given value, electrode failure can occur.

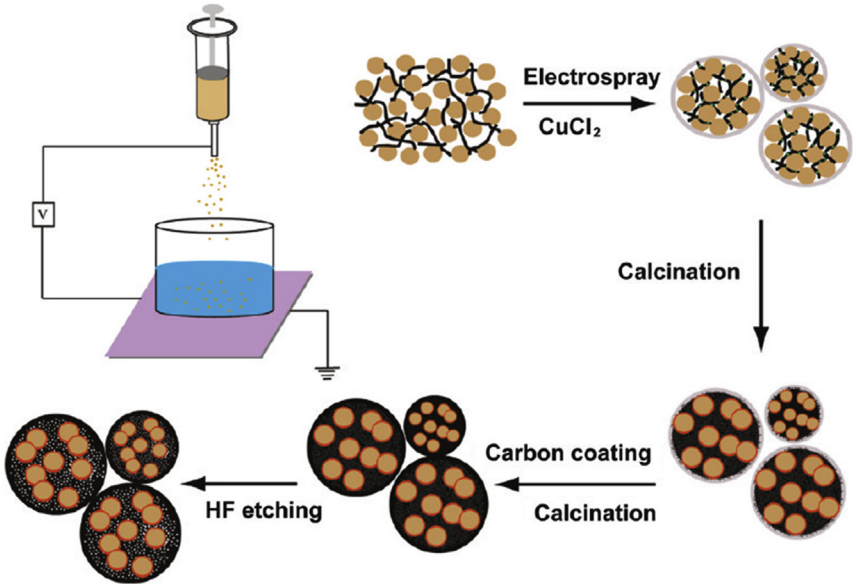

Fig. 5. Schematic representation of the programmed preparation of Si/C nanoporous microspheres. ©From Ref. [59].

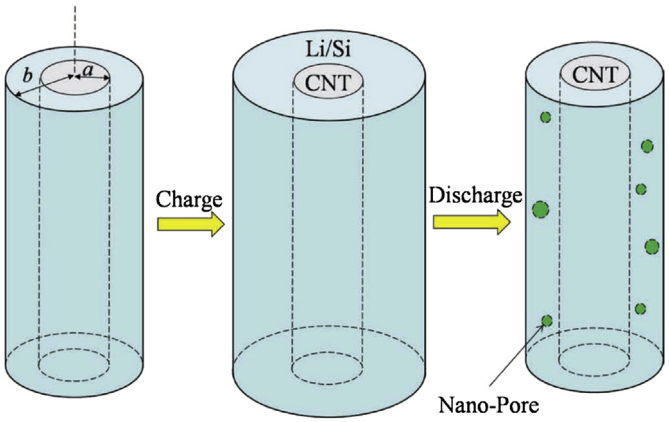

Fig. 6. Schematic illustration of the lithiation mechanism for a Si–C nanotube coaxial anode. During lithiation, the Si shell expands in the radial direction. During de-lithiation, nanopores form due to tensile stresses. ©From Ref. [60].

Magasinski et al. [12] illustrated a hierarchical bottom-up approach for the production of internally porous Si/C granules. The bottom-up synthetic technique begins with the annealing in a high-temperature furnace of carbon black nanoparticles and the formation of highly conductive branched structures. A CVD process is used to generate Si nanospheres inside the voids of the carbon structures. The Si/C nanospheres, mixed to graphitic carbon that acts as electrically conductive binder, self-assemble into rigid granules with sizes in the 10–30 micron range. The surface of a granule coated by Si/C nanospheres can be observed in the SEM image of Fig. 7. The composite granules are then used as anode material. The presence of a large number of interconnected pore channels inside the spheres enables a rapid entry of Li ions and provides accommodation for volume changes, avoiding anode cracking.

The concept of nanocomposite Si/C granules has been extended using high surface area multilayered graphene as support for nano-Si and C deposits [62]. Graphene sheets obtained from exfoliated natural graphite are coated by nanosized Si and by a thin C layer to decrease Si oxidation. SEM and TEM images of Si-coated graphene

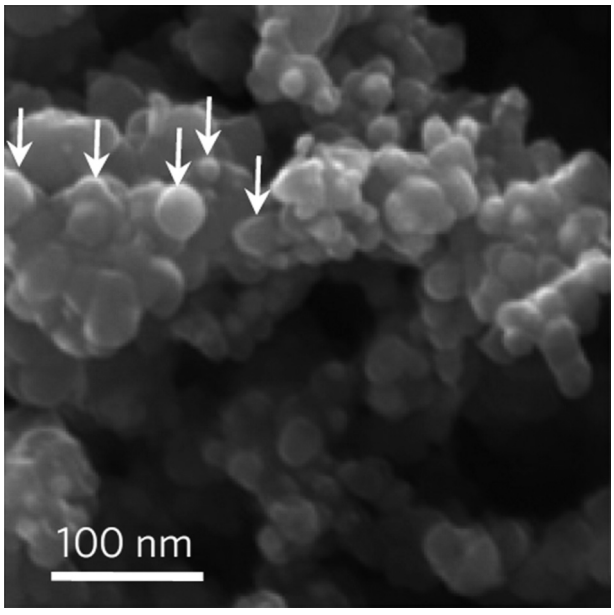

Fig. 7. SEM image of composite granules coated by Si/C nanospheres. ©From Ref. [12].

can be observed in Fig. 8. The continuous Si thin films deposited by CVD on the graphene sheets are able to accommodate volume changes via variation in thickness (Fig. 8c). The anodes assembled with this material exhibited a specific Li extraction capacity in excess of 2000 mAh g^{-1} at current density of 140 mA g^{-1} and stability over 150 cycles.

1.3. Si-coating of carbon nanostructures

Among the prominent fabrication processes, a successful one was the homogeneous deposition of Si nanoparticles (sizes: 10–20 nm) on fine graphitic particles [63]. The Si nanoparticles (10–20 nm) produced by pyrolysis of SiH_4 were homogeneously distributed on the surface of graphite. The electrochemical characterization of the compound material containing 7.1%$_{w/w}$ of Si revealed that the C and Si components were independently lithiated and de-lithiated and that the specific reversible capacity of the Si phase at the beginning of cycling exceeded 2500 mAh g^{-1}.

A strategy explored during the last few years deals with the coating by Si of tubular carbon nanostructures, such as carbon nanofibers (CNF) and CNT.

By using a conventional sputtering system, amorphous Si layers, with thickness in the 200–300 nm range, have been deposited on CNF films produced via the slurry spreading method [64]. The Si-coated CNF provide conducting pathways and strain/stress relaxation. The specific capacity of such materials was more than 2000 mAh g^{-1} and a good capacity retention after a large number (about 100) of cycles was detected.

A successful category of material has been obtained by a hierarchical structural approach that uses CNT to support silicon. The resulting material is mechanically robust, the diameter and spacing of the Si/C nanotubes can be controlled by the patterning of the catalyst used for the CNT growth. In the case of Si deposited on vertically aligned CNT architectures, the CNT act as a flexible mechanical support for strain release, offering efficient conducting channels.

Deposits of commercial multi-wall carbon nanotubes (MWCNT) have been coated with Si nanocrystals obtained by vaporization of Si targets in a mini-arc source [65]. The apparatus enables a rapid quenching of the silicon vapour and the produced Si nanocrystals (sizes around 5 nm) are carried out by an Ar flux. Using electrostatic forces the partially charged Si nanocrystals are then attached onto the MWCNT outer surfaces.

Arrays of CNT grown inside the pores of a template have been used to fabricate a coaxial CNT–silicon–carbon composite structure [66]. In this configuration the external carbon layer protects the SEI and acts as at the same time as current collector. The close contact of Si to CNT promotes direct and efficient charge transfer and enhances the device efficiency. An areal capacity of about 6 mAh cm^{-2} has been measured and this value results higher than the ones of commercial graphite anodes.

A template-free approach was used to produce Si/CNT vertically aligned heterostructures by a two-step CVD [67]. The first step generated CNTs (of the MWCNT type) arrays using xylene/ferrocene liquid mixtures; The second step used gaseous SiH_4/Ar mixtures to deposit Si nanoclusters (Fig. 9) that resulted tethered to the CNT surfaces by an amorphous carbon interface. These hybrid Si/CNT systems are characterized by a reversible capacity of about 2000 mAh g^{-1}, with a fade in capacity of about 15% per cycle.

1.4. C-coating of silicon nanostructures

An inverse approach to obtain hybrid Si–C materials is the coating of Si by nanocarbons. The coating of Si particles by carbon layers with various structural features has been achieved using

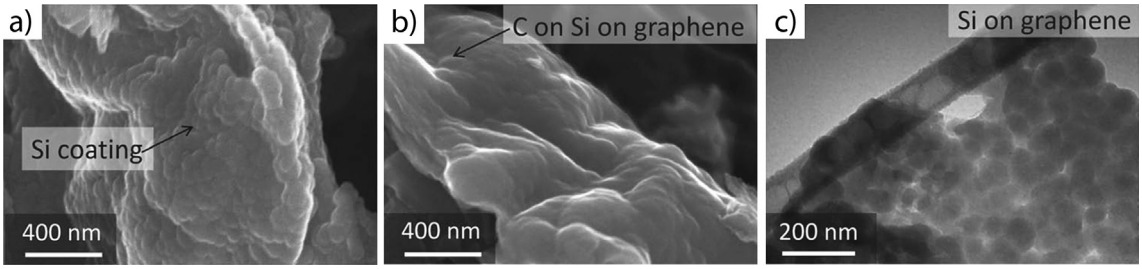

Fig. 8. SEM (a–b) and TEM (c) images of Si-coated graphene. In (c) the continuous Si film deposited on graphene is clearly evidenced. ©From Ref. [62].

different methodologies, such as thermal vapour deposition [39,68,69], chemical vapour deposition [70] or via carbonization of Si nanoparticles pre-coated with a variety of carbon precursors [31,46,58,71].

Decomposition of benzene vapour in a quartz tube furnace was used to coat Si particles (average size: 50 μm) with carbon particles (average size: 18 μm) [39]. For electrode fabrication the C-coated Si samples were grounded in a mortar and the downsized resulting powders were spread on copper foil substrates. The experiments carried out using this material, submitted to further thermal treatments, evidenced improvement of the electrochemical performances compared with those of uncoated Si and average working voltages lower than those of graphite. Moreover it was noted a satisfactory compatibility with both ethylene and propylene based electrolytes.

Surface coating of microsized Si powders by conductive granular C material deposited by CVD was found to reduce local fading modes associated with individual Si particles and to improve global stability against fading [70].

A versatile and industrial oriented approach to coat Si nanopowders with C has been proposed in Refs. [58,71]. Using this synthetic route, dispersions of nanosized Si particles in citric acid/ethanol are spray-pyrolyzed in air at temperatures between 300 and 500 °C. The low-temperature synthesis produces spheroidal crystalline Si nanoparticles coated by homogeneous amorphous C layers, whose thicknesses can be modulated by varying the process temperature. A TEM image of the C-coated Si nanoparticles and a high resolution TEM image showing the C–Si interface are reported in Fig. 10. This class of anode material is characterized by an excellent specific capacity retention (up to 1120 mAh g^{-1}).

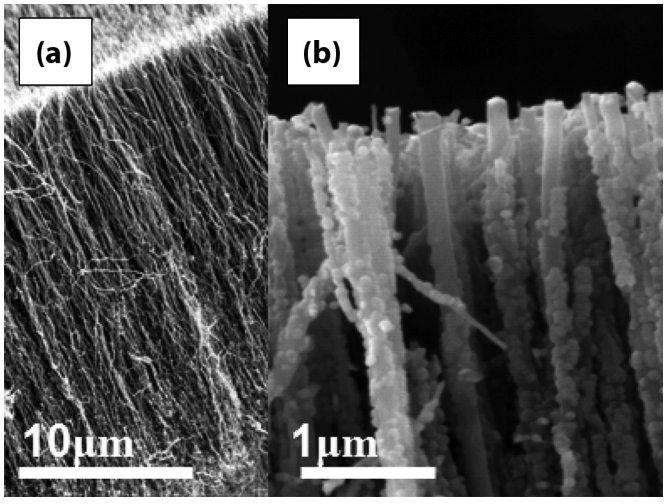

Fig. 9. SEM images of (a) aligned CNT arrays prior to Si deposition and (b) multiple clusters of CNT coated by Si nanoclusters. ©From Ref. [67].

Hydrothermal carbonization of glucose was instead used in Ref. [31] to fabricate Si–SiO_2/C systems. In this case the Si nanoparticles were coated with a thin layer (3–5 nm) of amorphous SiO_x and C. The uniform sphere-like particles, with a core–shell structure, were used as anode materials, obtaining stable reversible capacities. The improvement of the Li-storage properties has been ascribed to the formation of a stable SEI on the surface of the active particles.

Zhang et al. [54] prepared by CVD hybrid materials formed by CNT grown on Si nanoparticles. During the CNT growth a simultaneous deposition of pyrolytic carbon occurred, resulting in a coating by amorphous carbon of the whole CNT/Si systems. After 20 cycles this pyrolytic-carbon coated Si/CNT composite material achieved a discharge capacity of 727 mAh g^{-1}, about two times the value obtained by systems where the silicon and CNT were simply mechanically mixed before the pyrolytic coating. The improvement of cyclability has been ascribed to the ability of the CVD-grown CNT to sustain the integrity of the pyrolytic-carbon coated Si/CNT structures and to the maintenance of electrical connections.

An alternative configuration is that of hierarchical Si/C systems consisting of Si nanowire (SiNW) arrays coated by carbon (Fig. 11). Huang et al. [72] prepared carbon-coated SiNW arrays by metal catalytic etching of Si plates. The procedure of SiNW preparation was followed by addition of carbon aerogel and pyrolysis. This hybrid nanomaterial exhibited a first discharge capacity of 3344 mAh g^{-1} with a reversible capacity of 1326 mAh g^{-1} after 40 cycles. The good performances are ascribed to a better electronic contact/conduction and to an effective accommodation of Si volume changes provided by the carbon coating.

The concept of hierarchical C-on-Si systems has been recently further developed by one-step building of polycrystalline Si nanocones coated by either carbon nanotubes [73] or layers of hydrogenated amorphous carbon [74]. It has been demonstrated that a dual mode microwave/radio frequency plasma system can be used in order to activate kinetically driven processes able to create new chemistries and to open unexpected routes for integration of Si and C elements in hybrid nanostructures. The structural characteristics of such new hybrid Si/C nanomaterial are expected to be particularly suitable for their reliable use in Li-ion anodes. The special structural features of these complex 3D architectures offer a potential capability to increase electronic contact and conduction, and to buffer volume changes during the Li-ion intercalation processes.

1.5. Si/C core/shell

To accommodate large volume modifications, the introduction of void spaces between Si materials and the C-coatings has been recently proposed. A class of innovative core–shell carbon-on silicon anode material has been designed and tested.

Xu et al. [75] prepared core/shell structures starting from nanosized silicon dispersed in a polyvinylidene fluoride solution. The compounds were thereafter submitted to pyrolysis. The Si core

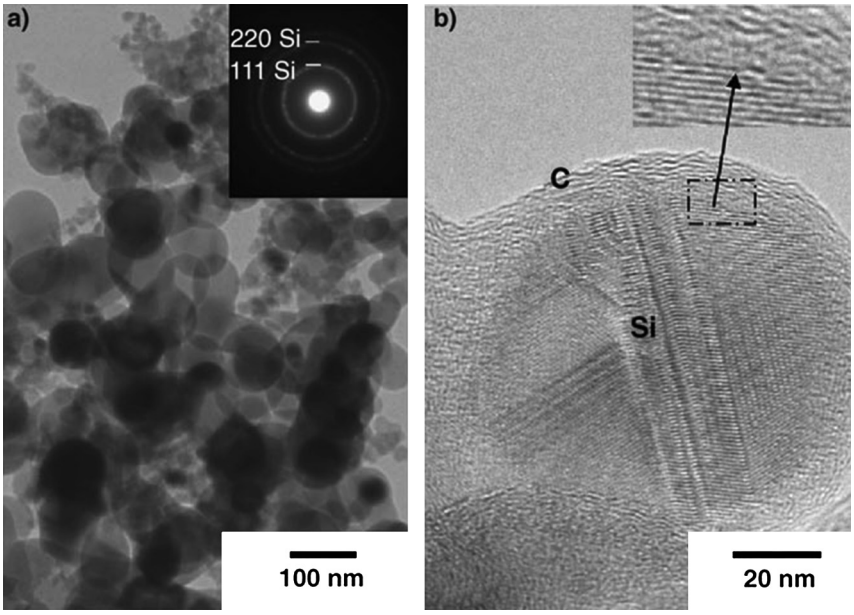

Fig. 10. (a) TEM image of spheroidal C-coated Si nanoparticles produced by spray pyrolysis in air. The indexed diffraction pattern in the inset confirms the presence of Si nanoparticles. (b) HR-TEM image of a C-coated Si nanoparticle. The inset evidences the interface between a crystalline Si particle and the external pyrolyzed C layer. ©From Ref. [58].

resulted coated by an amorphous C layer that enhanced the reversible capacity of the pristine Si, delivering a stable value of 450 mAh g^{-1} even at 1000 mA g^{-1}. The authors ascribed the improvements to the presence of the C shell, able to suppress agglomeration of the Si nanoparticles, and to buffer the volume changes. Following the same research line, porous Si/C nanocomposites characterized by a hollow core–shell structure have been designed and produced [76]. In this configuration Si nanoparticles surrounded by void space, are encapsulated in amorphous C spheres, with an intermediate SiO_2 layer. A schematic diagram of the synthesis process and TEM images of the hollow core–shell structures are shown in Fig. 12. The presence of large void space, up to tens of nanometers, allowed achieving a value of 86% capacity retention over 100 cycles.

Liu et al. [77] encapsulated Si nanoparticles in yolk-shell carbon prepared by the pyrolysis of thin polymer layers. The void space created inside the carbon hollow spheres helped in preventing the rupture of the C shell during volume expansion of Si, and improved the cycling stability allowing to reach up to 1000 cycles with an efficiency of about 99%.

A two-step coating method for modulation of the built-in buffer voids in Si core–hollow carbon shell nanocomposites has been proposed [78]. A systematic research work was carried out in order to investigate the influence of the void sizes on the electrochemical performances. The authors found that a void/Si volume ratio of about 3 is the best value to efficiently accommodate the Si volume expansion assuring at the same time good electrical contacts. The steps of the synthesis process that produce different built-in buffer voids are schematically indicated in Fig. 13.

Recently Si nanoparticles were also encapsulated by crumpled graphene shells [79]. The wrapping of Si was achieved by a capillary-driven assembly route, starting from dispersions of graphene oxide sheets and Si nanoparticles nebulized to form aerosol droplets and heated in a tube furnace. Compared with the pristine Si nanoparticles, the hybrid C/Si capsules showed greatly enhanced electrochemical performances, with higher coulombic efficiency and slower capacity fade. The findings demonstrate the effectiveness of Si encapsulated inside hollow C spheres in accommodating Si volume changes and avoiding SEI deposition on the Si surface.

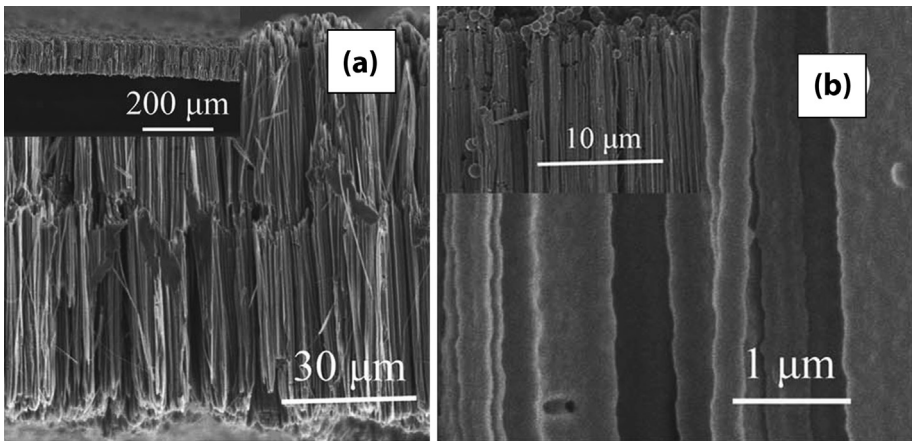

Fig. 11. Cross-section SEM images of (a) pristine SiNW film and (b) the C-coated SiNW film. ©From Ref. [72].

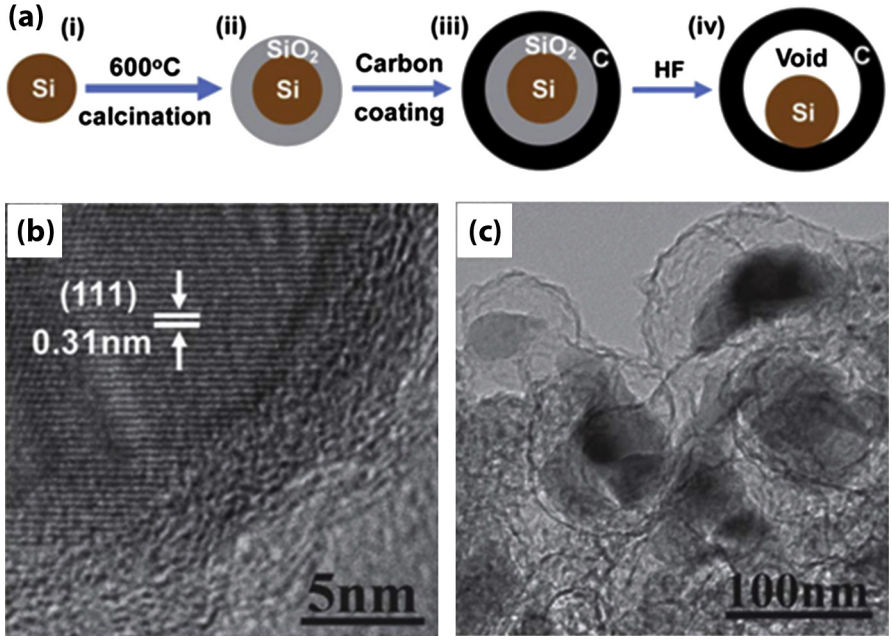

Fig. 12. Core–shell porous Si–C nanocomposites. (a) Schematic diagram of the synthesis process; (b–c) TEM images of $Si/SiO_2/C$ nanocomposites: (b) after the C coating and (c) after the HF etching removing the SiO_2 in-between layer. ©From Ref. [76].

As regards the thickness of the external C shell in C/Si core shell configurations, the results of a systematic research performed by J.G. Zhang and co-workers within the DOE Vehicle Technologies Program [80] indicate that a C shell of about 80 nm is able to assure the integrity of a 50 nm Si core after lithiation.

1.6. *In situ* studies

A specific mention must be given to some recent papers that report *in situ* investigations of Si/C nanostructured anode materials under working conditions. The team led by Wang et al. [81] prepared an anode material consisting in carbon fibres coated by amorphous Si and investigated the phase transformation and microstructural evolution of the composite material during the charge/discharge processes. The *in situ* TEM imaging of the electrode during the battery's operation was made possible by the reduced dimensions of the assembled Li-ion battery. The structural/morphological study of the battery under working conditions, coupled with a molecular dynamic calculation approach, enabled to reveal in real time details at the micro-nanoscale of how the anode material operates and how repeated use could wear the electrode down. In particular the investigation confirmed some hypotheses that were long been postulated, as the about 300% swelling of the Si phase. Moreover the study highlighted some unexpected effects, as the cyclic formation of unstructured Si/Li glassy phase and of an unconventional crystallization process, known as congruent phase transition.

The same experimental/computational approach was used to investigate a different type of Si/C anode material, consisting this time of Si nanoparticles anchored to the external surface of carbon nanofibers or embedded inside a fibre [82]. The goal of this study was to understand the mechanism of Li ions transport across a

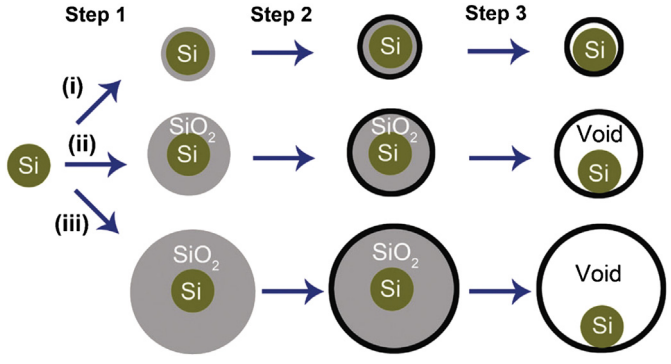

Fig. 13. Scheme of the process that produces silicon core–hollow carbon shell nanocomposites with 3 different buffer voids between Si core and C shell. ©From Ref. [78].

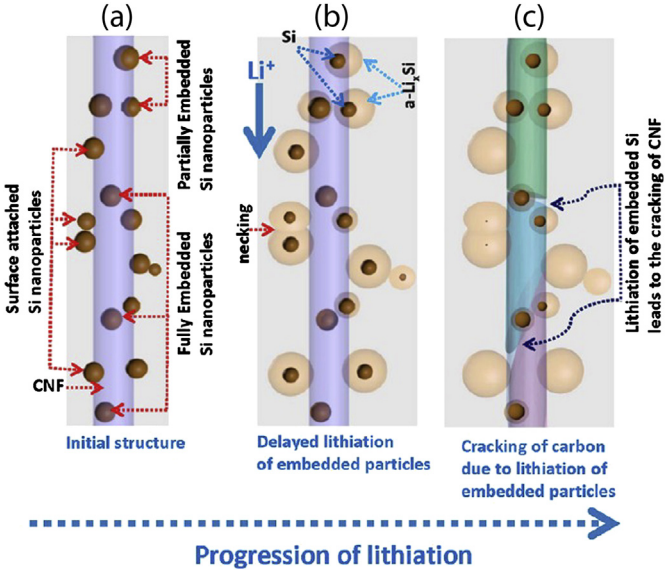

Fig. 14. Schematic drawing of the lithiation characteristics of the Si nanoparticles attached to or embedded in carbon nanofibers (CNF). (a) Initial structure; (b) lithiation of the Si particles embedded in the CNF is delayed as compared with the Si particles attached to the CNF surface; (c) lithiation of the embedded Si particles leads to CNF cracking. ©From Ref. [82].

Table 1
The table classifies in few significantly different classes the various Si/C materials obtained through the use of various technologies. The most significant results for their use in Li-ion anodes are also reported.

Class of materials	Employed technologies [Refs.]	Highest capacitances obtained (mAh g^{-1})		Current density (mA g^{-1})	Properties degradation
Nanocomposites without a defined structure (mixtures, dispersions, etc.)	Milling [49,50,53] Milling/heating [43,44,48,54]	970	Si–C	NA	Capacity fade 0.24%, during 40 cycles
	Pyrolysis [10,45,47] Vapour decomposition [51,52]	2274	Si–CNT	NA	727 mAh g^{-1} after 20 cycles
Porous structures	Carbonization [56]	1600	Porous	100	1280 mAh g^{-1} after 118 cycles
	CVD [12,60–62] Electrospraying [59] Mechanochemical [55] Pyrolysis [46] Spray-pyrolysis [58] VLS growth [57]	2800	Sponge-like	140	1300 mAh g^{-1}
C coated by Si	CVD [63,66,67]	>2500	Graphite	NA	1900 mAh g^{-1} after 100 cycles
	Plasma vaporization [65] Sputtering [64]	2000	CNT	NA	15% fade capacity/cycle
Si coated by C	CVD [54,68,73] Hydrothermal carbonization [31] Spray-pyrolysis [58,71,72] Thermal vapour decomposition [39]	3344		1000	1490 mAh g^{-1} after 20 cycles
Core–shell with void spaces	Calcination [76] Milling [80] Pyrolysis [75,77] Solution chemistry [78,79]	1200		1000	450 mAh g^{-1}

composite Si/C system. The results demonstrated the different lithiation behaviour of the Si particles externally attached to the C nanofibres and of those embedded in the carbon matrix. In this last case lithiation of the Si nanoparticles can easily produce fractures of the fibre. A scheme showing the lithiation behaviour of the differently located nanoparticles is presented in Fig. 14.

2. Conclusions

For the development of more efficient Li-ion batteries, anode fabrication is moving from the use of C or Si to that of Si–C hybrid materials, able to compensate for the limitations related to each of such elements taken alone. A stringent reasoning about advantages and drawbacks of using pure Si and graphite for Li-ion anodes is found in the paper by Wu and Bennett [83].

The present paper surveys state-of-the-art of materials design and the most promising approaches to produce new exciting families of Si/C anode materials with increased mass capacity, energy density and cycling stability.

The most significant results obtained for the Si/C materials have been classified in few classes and are summarized in Table 1. Considering the large variety of the used techniques and of the corresponding experimental set-up, the data reported in the literature are characterized by a significant spread of the values, strongly depending on the specific parameters process. In such a context the reported data in the literature cannot be strictly compared and only a their grouping 'at large' can be considered useful, being roughly indicative of the functional properties of the synthesized materials.

The synthesis strategies carried out in laboratories around the world span from pyrolysis to spraying, from sputtering to hydrothermal reactions, from plasma-aided processes to chemical vapour deposition. The first consideration is that the use of materials at the nano-scale enables in general to overcome some drawbacks accompanying the anodes made by the same materials at micro-macro-scale. This holds in general for pure C and pure Si structures, but also when a combination of such elements is involved. However, downsizing in matter is not able by itself to guarantee noticeable performance improvements. One must indeed consider that the electrode functionality calls into play both electron mobility and ions mobility and therefore requires a complex design of the nanomaterial structure. On one hand, good crystallinity is needed for efficient electron transport in the solid state, on the other hand controlled porosity to assure high ion mobility, and it is not easy to find a feasible solution for such seemingly conflictual concepts.

It is demonstrated that either a single blend of nanosized C and Si, or Si/C nanocomposites produced by mechanical milling, cannot satisfactory solve the problem of capacity fading on cycling. This finding supports the hypothesis that only arrangements of Si–C bi-component nanostructures in well-defined architectures can assure real benefits. In effect, significant improvements in cycling stability, but also in capacity and energy density, have been reached when rationally designed intercalation materials based on Si–C coupling have been converted into practical forms.

A critical analysis of the data indicates that the deliberate design and subsequent tailoring by hierarchical bottom-up approaches of nanoporous Si/C systems, of Si nanostructures coated by C and C nanostructures coated by Si, and of core–shell heterostructures, provide a way towards technologically relevant capacities, much higher than those of conventional carbon. The results obtained so far clearly evidence that no radical changes in the battery structure are required, but rather that significant advantages in the battery performances can be ensured by a proper design of the material and a judicious engineering of the electrode.

At this stage, it is not possible to extract from the reported data the indication of a preferential direction along which to move, because all the proposed Si/C configurations offer viable options to solve in principle the main problems of the conventional anodes, but not all the configurations can be easily scaled up to an industrial level. However it must be noted that some of the above reported intriguing Si/C nanostructures could find suitable applications also in other advanced technological fields, such as in field emission based devices [84], light-emitting diodes [85] and solar cells [65].

References

[1] K. Kang, Y.S. Meng, J. Breger, C.P. Grey, G. Ceder, Science 311 (2006) 977–980.
[2] M. Armand, J.M. Tarascon, Nature 451 (2008) 652–657.
[3] B. Scrosati, J. Garche, J. Power Sources 195 (2010) 2419–2430.
[4] J.M. Tarascon, M. Armand, Nature 414 (2001) 359–367.

[5] M. Yoshio, T. Tsumura, N. Dimov, J. Power Sources 146 (2005) 10–14.
[6] C. Liu, F. Li, L.P. Ma, H.M. Cheng, Adv. Mater. 22 (2010) E8–E62.
[7] R. Marom, S.F. Amalraj, N. Leifer, D. Jacob, D. Aurbach, J. Mater. Chem. 21 (2011) 9938–9954.
[8] M.N. Obrovac, L. Christensen, Electrochem. Solid-State Lett. 7 (2004) A93–A96.
[9] H. Wu, Y. Cui, Nano Today 7 (2012) 414–429.
[10] J.J. Wu, W.R. Bennet, in: Proceeding IEEE Energy Tech 2012, 2012, pp. 1–5.
[11] M. Holzapfel, H. Buqa, W. Scheifele, P. Novak, F.M. Petrat, Chem. Commun. 12 (2005) 1566–1568.
[12] A. Magasinski, P. Dixon, B. Hertzberg, A. Kvit, J. Ajala, G. Yushin, Nat. Mater. 9 (2010) 353–358.
[13] H. Kim, B. Han, J. Choo, J. Cho, Angew. Chem. Int. Ed. 47 (2008) 10151–10154.
[14] J. Cho, J. Mater. Chem. 20 (2010) 4009–4014.
[15] J. Zhu, C. Gladden, N. Liu, Y. Cui, X. Zhang, Phys. Chem. Chem. Phys. 15 (2013) 440–443.
[16] H. Li, X. Huang, L. Chen, Z. Wu, Y. Liang, Electrochem. Solid-State Lett. 2 (1999) 547–549.
[17] B. Gao, S. Sihna, L. Fleming, O. Zhou, Adv. Mater. 13 (2001) 816–819.
[18] H. Ma, F. Cheng, J. Cheng, J. Zhao, C. Li, Z. Tao, J. Liang, Adv. Mater. 19 (2007) 4067–4070.
[19] C.K. Chan, H. Peng, G. Liu, K. Mcllwrath, X.F. Zhang, R.A. Huggings, Y. Cui, Nat. Nanotechnol. 3 (2008) 31–35.
[20] M.H. Park, M.G. Kim, K. Kim, J. Kim, S. Ahn, Y. Cui, J. Cho, Nano Lett. 9 (2009) 3844–3847.
[21] T. Song, J. Xia, J.H. Lee, D.H. Lee, M.S. Kwon, J.M. Choi, J. Wu, S.K. Doo, H. Chang, W.I. Park, D.S. Zang, H. Kim, Y. Huang, K.C. Hwang, J.A. Rogers, U. Paik, Nano Lett. 10 (2010) 1710–1716.
[22] H. Kim, M. Seo, M.H. Park, J. Cho, Angew. Chem. Int. Ed. 49 (2010) 2146–2149.
[23] F. Cui, L. Hu, J.W. Choi, Y. Cui, ACS Nano 4 (2010) 3671–3678.
[24] S. Zhou, X.H. Liu, D.W. Wang, Nano Lett. 10 (2010) 860–863.
[25] Y. Yao, M.M. McDowell, I. Ryu, H. Wu, N. Liu, L. Hu, W.D. Nix, Y. Cui, Nano Lett. 11 (2011) 2949–2954.
[26] N.S. Choi, K.H. Yew, H. Kim, S.S. Kim, W.U. Choi, J. Power Sources 172 (2007) 404–409.
[27] J.H. Kim, H. Kim, H.J. .Sohn, Electrochem. Commun. 7 (2005) 557–561.
[28] P. Zuo, G. Yin, X. Hao, Z. Yang, Y. Ma, Z. Gao, Mater. Chem. Phys. 104 (2007) 444.
[29] D.C. Johnson, J.M. Mosby, S.C. Riha, A.L. Prieto, J. Mater. Chem. 20 (2010) 1993.
[30] Y. .You, L. Gu, C. Zhu, S. Tsukimoto, P.A.V. Aken, J. Maier, Adv. Mater. 22 (2010) 1.
[31] H.S. Hu, R. Demir-Cakan, M.M. Titirici, J.O. Muller, R. Schögl, M. Antonietti, J. Maier, Angew. Chem. Int. Ed. 47 (2008) 1645.
[32] P. Gao, J. Fu, J. Yang, R. Lv, J. Wang, Y. Nuli, X. Tang, Phys. Chem. Chem. Phys. 11 (2009) 11101.
[33] A.M. Wilson, G. Zank, K. Eguchi, W. Xing, J.R. Dahn, J. Power Sources 68 (1997) 195.
[34] W. Xing, A.M. Wilson, K. Eguchi, G. Zank, J.R. Dahn, J. Electrochem. Soc. 144 (1997) 2410.
[35] C.S. Wang, G.T. Wu, X.B. Zhang, Z.F. Qi, W.Z. Li, J. Electrochem. Soc. 145 (1998) 2751.
[36] D. Larcher, C. Mudalige, A.E. George, V. Portee, M. Gharghouri, J.R. Dahn, Solid State Ionics 122 (1999) 71.
[37] J. Yang, M. Wachtler, M. Winter, J.O. Besenhard, Electrochem. Solid-State Lett. 2 (1999) 161.
[38] N. Kurita, M. Endo, Carbon 40 (2002) 253.
[39] M. Yoshio, H. Wang, K. Fukuda, T. Umeno, N. Dimov, Z. Ogumi, J. Electrochem. Soc. 149 (2002) A1598.
[40] J. Saint, M. Morcrette, D. Larcher, L. Laffont, S. Beattie, J.P. .Peres, D. Talaga, M. Couzi, J.M. Tarascon, Adv. Funct. Mater. 17 (2007) 1765–1774.
[41] H. Kim, J. Cho, Nano Lett. 8 (2008) 3688–3691.
[42] B. Hertzberg, A. Alexeev, G. Yushin, J. Am. Chem. Soc. 132 (2010) 8548–8549.
[43] Y. Liu, K. Hanai, J. Yang, N. Imanishi, A. Hirano, Y. Takeda, Electrochem. Solid-State Lett. 7 (2004) A369–A372.
[44] X.W. Zhang, P.K. Patil, C. Wang, A.J. Appleby, F.E. Little, D.L. Cocke, J. Power Sources 125 (2004) 206–213.
[45] Y. Liu, Y. Wen, X.Y. Wang, A. Hirano, N. Imanishi, Y. Takeda, J. Power Sources 189 (2009) 733–737.
[46] Q. Si, K. Hanai, N. Imanishi, M. Kubo, A. Hirano, Y. Takeda, Q. Yamamoto, J. Power Sources 189 (2009) 761–765.
[47] Z.S. Wen, J. Yang, B.F. Wang, K. Wang, Y. Liu, Electrochem. Commun. 5 (2003) 165–168.
[48] H. Uono, B.C. Kim, T. Fuse, M. Ue, J.I. Yamaki, J. Electrochem. Soc. 153 (2006) A1708–A1713.
[49] H. Dong, R.X. Feng, X.P. Ai, Y.L. Cao, H.X. Yang, Electrochem. Acta 49 (2004) 5217–5222.
[50] P. Zuo, G. Yin, Y. Ma, Electrochim. Acta 52 (2007) 4878–4883.
[51] T. Ishiara, M. Nakasu, M. Yoshio, H. Nishiguchi, Y. Takita, J. Power Sources 146 (2005) 161–165.
[52] Z.O. Guo, Z.W. Zhao, H.K. Liu, S.X. Dou, Carbon 43 (2005) 1392–1399.
[53] Y. Zhang, X.G. Zhang, H.L. Zhang, Z.G. Zhao, F. Li, C. Liu, H.M. Cheng, Electrochim. Acta 51 (2006) 4994–5000.
[54] Y. Zhang, Z.G. Zhao, X.G. Zhang, H.L. Zhang, F. Li, C. Liu, H.M. Cheng, Int. J. Nanomanuf. 2 (2008) 4–15.
[55] X. Feng, J. Yang, P. Gao, J. Wang, Y. Nuli, RSC Adv. 2 (2012) 5701–5706.
[56] J. Guo, X. Chen, C. Wang, J. Mater. Chem. 20 (2010) 5035–5040.
[57] S. Hwak, J.H. Park, S.W. Hwang, D. Whang, J. Electrochem. Soc. 159 (2012) A1273–A1277.
[58] S.H. Ng, J. Wang, D. Wexler, K. Kostantinov, Z.P. Guo, H.K. Liu, Angew. Chem. Int. Ed. 45 (2006) 6896–6899.
[59] Y.X. Yin, S. Xin, Li.J. Wan, C.J. Li, Y.G. Guo, J. Phys. Chem. C 115 (2011) 14148–14154.
[60] L. Hu, H. Wu, Y. Gao, A. Cao, H. Li, J. McDough, X. Xie, M. Zhou, Y. Cui, Adv. Energy Mater. 1 (2011) 523–527.
[61] X.C. Gui, J.Q. Wei, K.L. Wang, A.Y. Cao, H.W. Zhu, Y. Jòia, Q.K. Shu, D.H. Wu, Adv. Mater. 22 (2010) 617–621.
[62] K. Evanoff, A. Magasinski, J. Yang, G. Yushin, Adv. Energy Mater. 1 (2011) 495–498.
[63] M. Holzapfel, H. Buqa, F. Krumeich, P. Novak, F.M. Petrat, C. Veit, Electrochem. Solid-State Lett. 8 (2005) A516–A520.
[64] P.C. Chen, J. Xu, H. Chen, C. Zhou, Nano Res. 4 (2011) 290–296.
[65] M. Liu, G. Lu, J. Chen, Nanotechnology 19 (2008) 265705 (5pp.).
[66] C. Zhao, Q. Li, W. Wan, J. Li, J. Li, H. Zhou, D. Xu, J. Mater. Chem. 22 (2012) 12193–12197.
[67] W. Wang, P.N. Kumta, ACS Nano 4 (2010) 2233–2241.
[68] N. Dimov, K. Fukuda, T. Umeno, S. Kugino, M. Yoshio, J. Power Sources 114 (2003) 88–95.
[69] X.Q. Yang, J. McBreen, W.S. Yoon, M. Yoshio, H.Y. Wang, K.J. Fukuda, T. Umeno, Electrochem. Commun. 4 (2002) 893–897.
[70] W.R. Liu, J.H. Wang, H.C. Wu, D.T. Shieh, M.H. Yang, N.L. Wu, J. Electrochem. Soc. 152 (2005) A1719–A1725.
[71] S.H. Ng, J. Wang, D. Wexler, S.Y. Chew, H.K. Liu, J. Phys. Chem. C 111 (2007) 11131–11138.
[72] R. Huang, X. Fan, W. Shen, J. Zhu, Appl. Phys. Lett. 95 (2009) 133119–133119-3.
[73] F. .Toschi, S. Guglielmotti, I. Cianchetta, C. Magni, M.L. Terranova, M. Pasquali, E. Tamburri, R. Matassa, M. Rossi, Chem. Phys. Lett. 539–540 (2012) 94–101.
[74] S. Orlanducci, F. Toschi, V. Guglielmotti, I. Cianchetta, C. Magni, E. Tamburri, M.L. Terranova, R. Matassa, M. Rossi, Cryst. Growth Des. 12 (2012) 4473–4478.
[75] Y. Xu, G. Yin, Y. Ma, P. Zuo, X. Cheng, J. Mater. Chem. 20 (2010) 3216–3220.
[76] X. Li, P. Meduri, X. Chen, W. Qi, M.H. Engelhard, W. Xu, F. Ding, J. Xiao, W. Wang, C. Wang, J.G. Zhang, J. Liu, J. Mater. Chem. 22 (2012) 11014–11017.
[77] N. Liu, H. Wu, M.T. Mc Dowell, Y. Yao, C. Wang, Y. Cui, Nano Lett. 12 (2012) 3315–3321.
[78] S. Chen, M.L. Gordin, R. Yi, G. Howlett, H. Sohn, D. Wang, Phys. Chem. Chem. Phys. 14 (2012) 12741–12745.
[79] J. Luo, X. Zhao, J. Wu, H.D. Jang, H.H. Kung, J. Huang, Phys. Chem. Lett. 3 (2012) 1824–1829.
[80] DOE Vehicle Technologies Program, 2012. Report.
[81] M. Wang, X. Li, Z. Wang, W. Xu, J. Liu, F. Gao, L. Kovarik, J.G. Zhang, J. Howe, D.J. Burton, A. Liu, X. Xiao, S. Thevuthasan, R.R. Baer, Nano Lett. 12 (2012) 1624–1632.
[82] M. Gu, Y. Li, S. Hu, X. Zhang, W. Xu, S. Thevuthasan, D.R. Baer, J.G. Zhang, J. Liu, C.M. Wang, ACS Nano 6 (2012) 8439–8447.
[83] J.J. Wu, W.R. Bennett, 2012 IEEE Energy Tech Conference, 29–31 May 2012. Cleveland, OH, United States, (also as NASA report: E-18273).
[84] Y. Liu, S. Fan, Solid State Commun. 133 (2005) 131–134.
[85] S. Kamiyama, M. Iwaya, T. Takeuchi, I. Akasaki, R. Yakimova, M. Syväjärvi, Thin Solid Films 522 (2012) 23–25.